

Electronic Supplementary Information

Direct deposition of MoSe₂ nanocrystals on metallic substrates: Towards ultra-efficient electrocatalysts for hydrogen evolution

Dijo Damien,^a Athira Anil,^a Dipanwita Chatterjee^b and M. M. Shaijumon^{a}*

^aIndian Institute of Science Education and Research Thiruvananthapuram,
Thiruvananthapuram, Kerala, 695016, India.

^bMaterials Research Center, Indian Institute of Science, Bangalore, Karnataka, 560012, India.

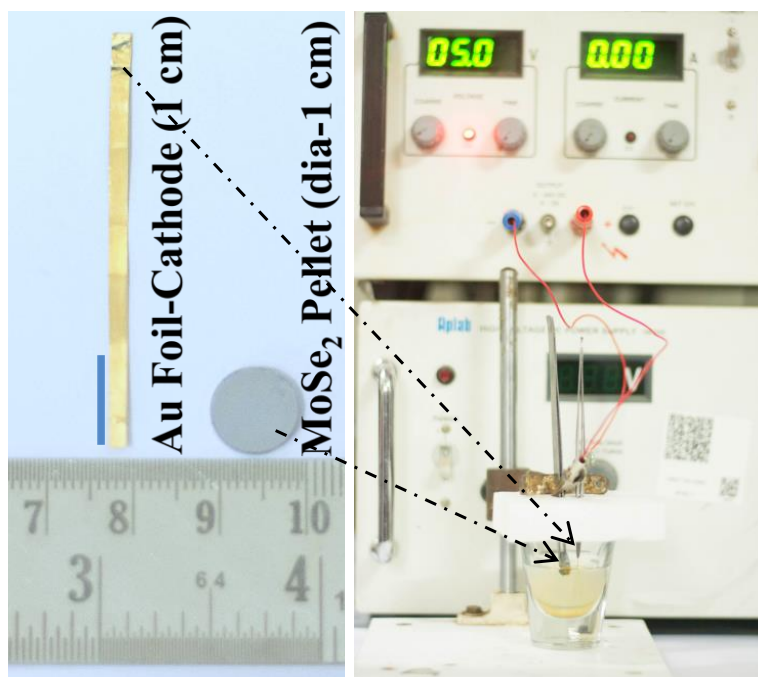


Fig. S1: Photographs of the electrodes and the experimental set up used for the electrochemical exfoliation and electrophoretic deposition of MoSe₂ nanocrystals onto Au foil.

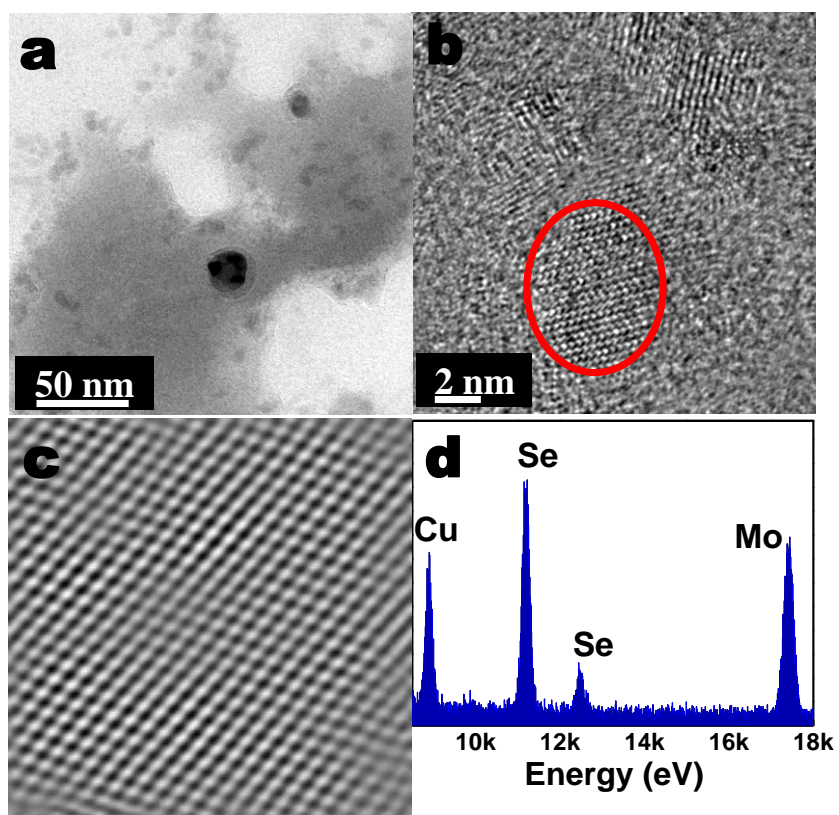


Fig. S2: **a.** Low magnification image of MoSe₂, with small grains of different contrast on the fuzzy sheets of MoSe₂, **b.** high resolution image of one of the grains and the corresponding IFFT image is shown in **c.** STEM-EDX spectrum acquired from the nanograins shown in **d,** exhibits an elemental composition of 1.3 : 1 , molybdenum to selenium.

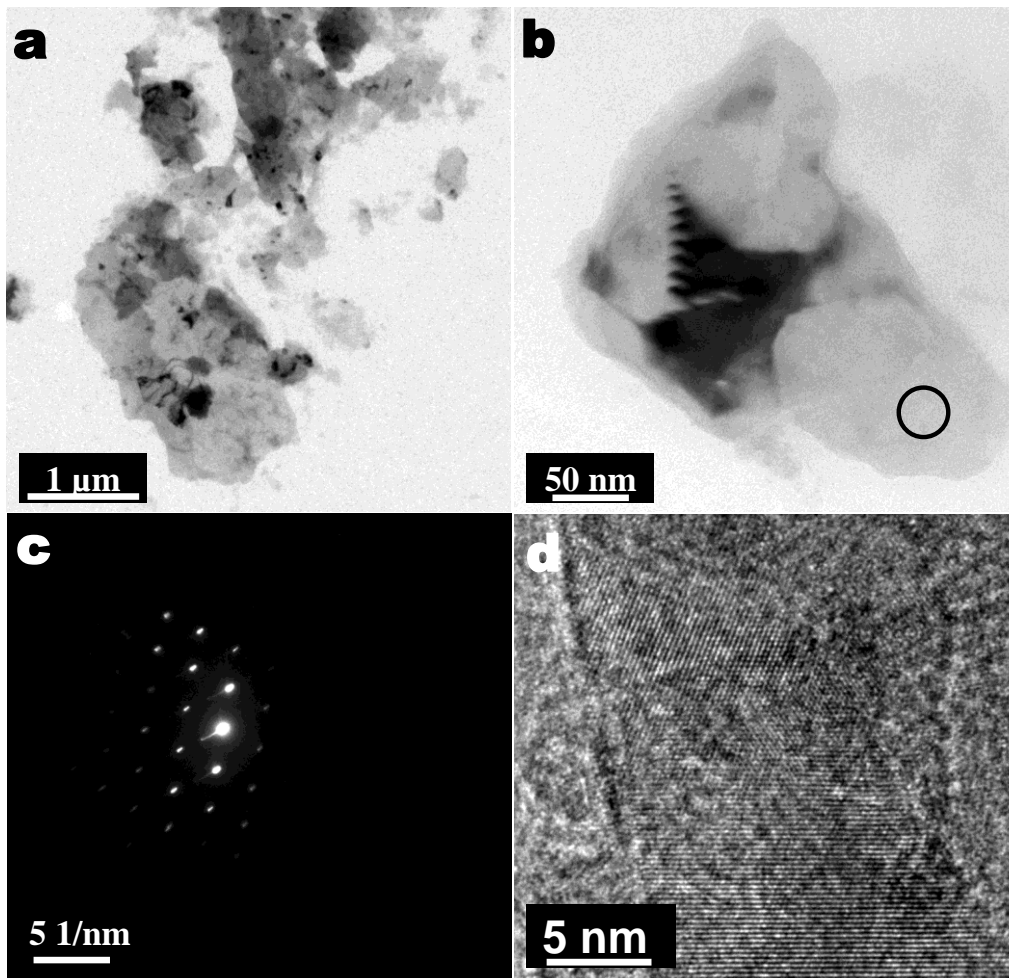


Fig. S3: **a** and **b**, Low magnification images of sheets of MoSe₂ present in the sample. Hexagonal nanobeam electron diffraction pattern acquired from the marked area in **b** is shown in **c** corresponding to 2H phase. However, HR-TEM image of the sheets shown in **d** clearly shows the presence of MoSe₂ nanocrystals with different lattice orientations.

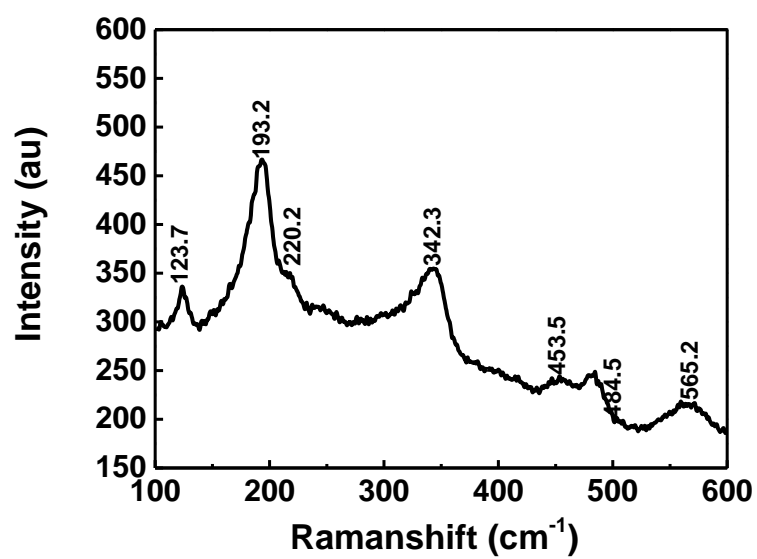


Fig. S4: Raman spectra of ED MoSe₂ sample show the presence of oxygen deficient oxides of Mo (MoO_{3-x}).

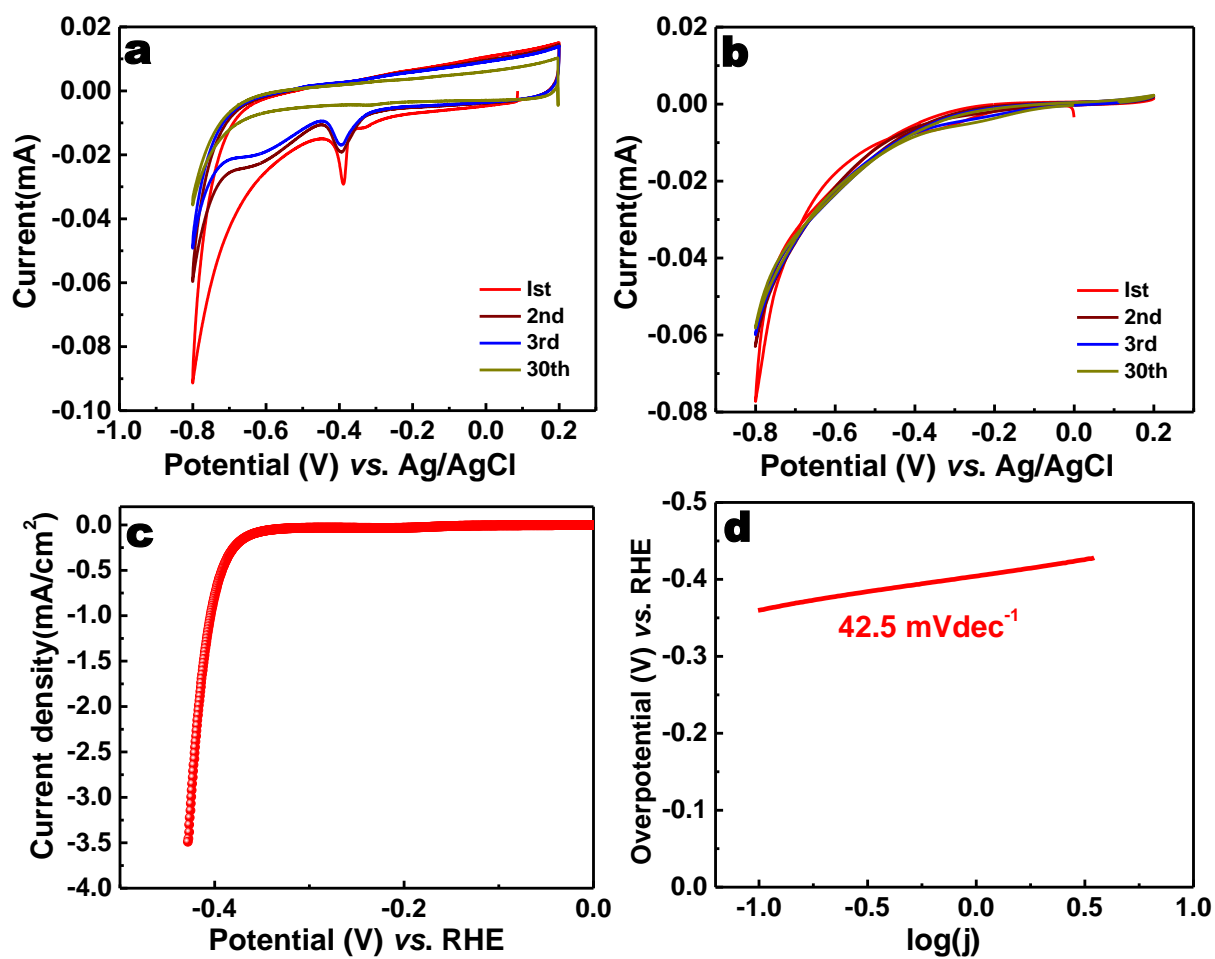


Fig. S5: Cyclic Voltammograms of **a**, MoSe₂ electrochemically exfoliated solution drop casted on gold working electrode and **b**, ED MoSe₂ electrode, in sodium phosphate buffer solution (pH = 7) at a scan rate of 100 m Vs⁻¹. **c** and **d**, respectively represent the polarization curve and Tafel plot of the drop casted electrodes in 0.5 M H₂SO₄ at a scan rate of 2 mV s⁻¹.

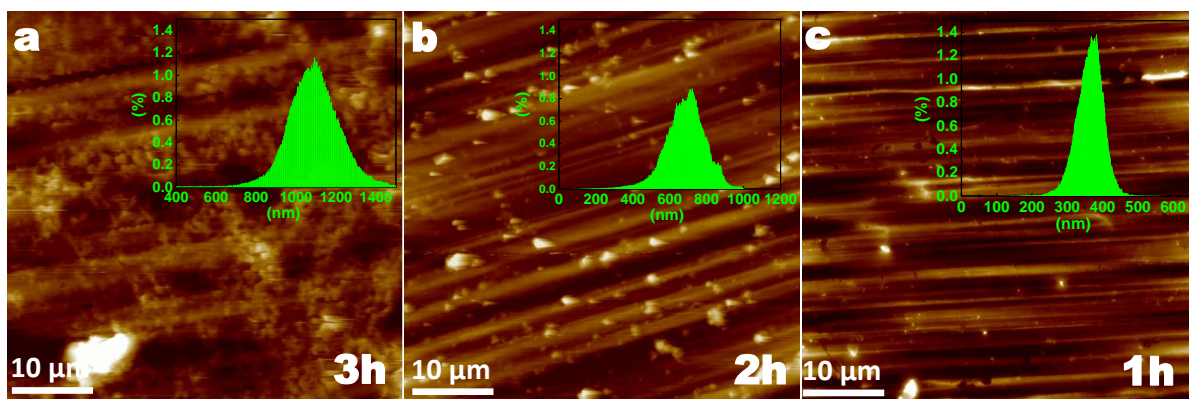


Fig. S6: Morphology and thickness of the **ED** MoSe₂ sample on gold foil is analysed using AFM. The active material coverage and the thickness of deposition drastically changes at regular intervals of time specified *viz.* 1h, 2h and 3h as shown in **a**, **b** and **c**, respectively. Inset of each figure shows depth correlation on the entire scanned area for the corresponding deposition time.

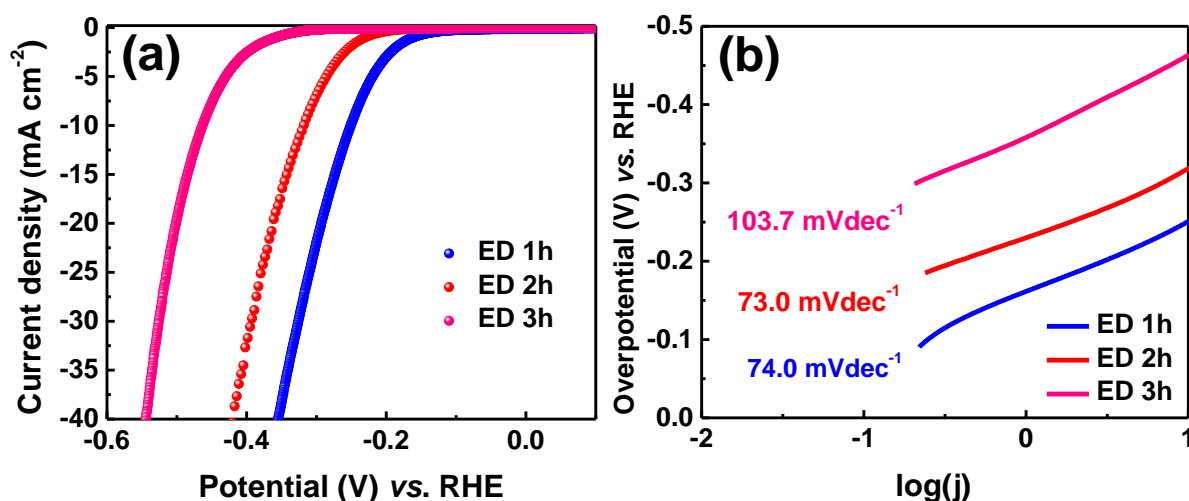


Fig. S7: Though the mass loading of the active material is irrelevant for the earth abundant catalysts like transition metal dichalcogenides, the optimization of thickness becomes important as it affects the kinetics of the catalysis reaction critically. Here, **a** represents the polarization curves obtained for **ED** samples fabricated for different deposition time as indicated in the figure at a sweep rate of 2 m Vs⁻¹ in 0.5 M H₂SO₄, and **b** represents the corresponding Tafel slopes.

Table S1. Evolution of elemental composition of constituting elements of LiTFSI in **ED 1h**, **ED 1h P1**, **ED 1h P2** and **ED 1h P3** electrodes. As the immersion time increases, percentage composition of Li increases and the organic components leech off.

Sample	At %					
	Li 1s	C 1s	N 1s	O 1s	F 1s	S 2p
Exfoliated solution	16.2	16.7	6.2	31.2	19.8	10.1
ED 1h	27.5	46.7	4.7	21.1	-	-
ED 1h P1	84.6	12.24	0.5	2.7	-	-
ED 1h P2	86.0	10.74	0.2	2.9	-	-
ED 1h P3	88.3	9.1	0.3	2.3	-	-

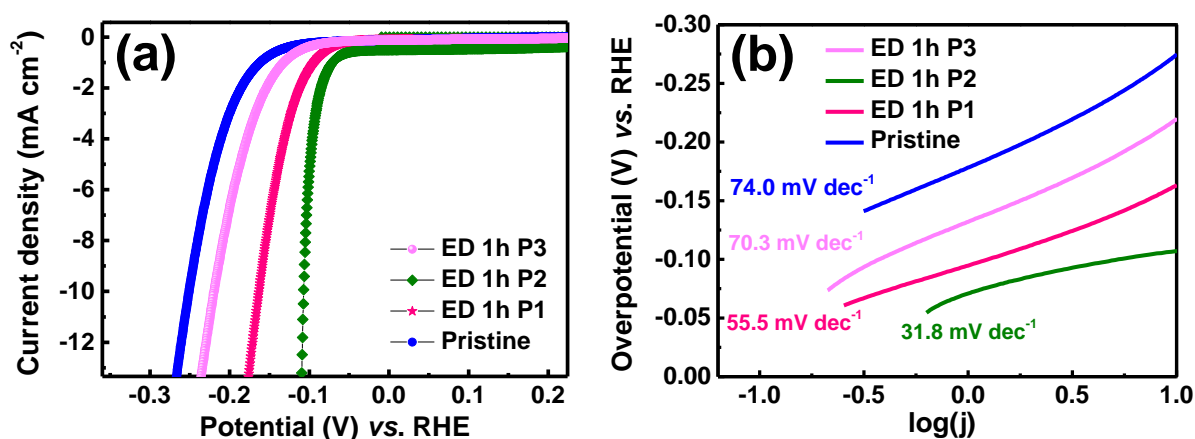


Fig. S8: Oxidation by piranha solution is a very well established route for the surface cleaning of many substrates for different applications. **ED 1h** electrode is dipped in freshly prepared piranha solution for 20 sec, 40 sec and 60 sec, respectively, to yield electrodes namely **ED 1h P1**, **ED 1h P2** and **ED 1h P3**. **a**, Polarization curves show **ED 1h P2** gives the best electrochemical performance. Tafel plots for the four electrodes are shown in **b**.

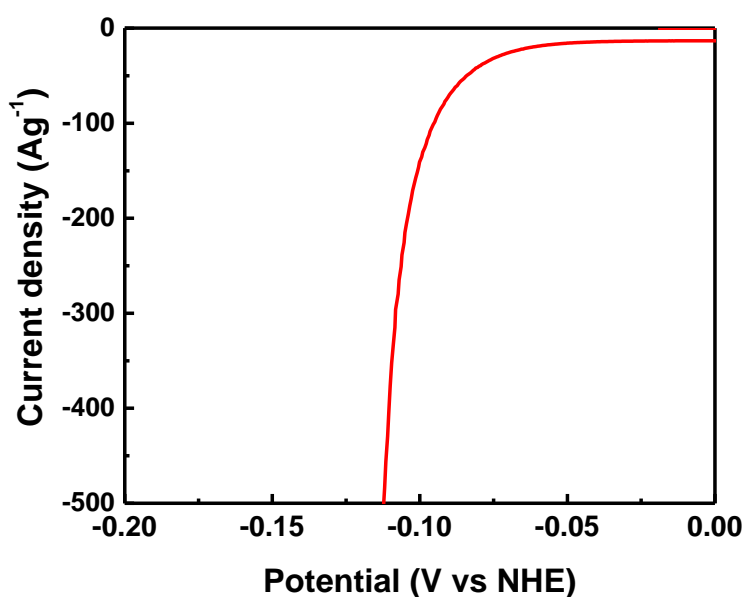


Fig. S9: Polarization curve obtained for the best performing electrocatalyst- **ED 2h P2** in terms of gravimetric current density. However, higher mass loading will result in feeble electron- proton communication and end up reduced catalytic activity as evident from the experiments varying the deposition time.

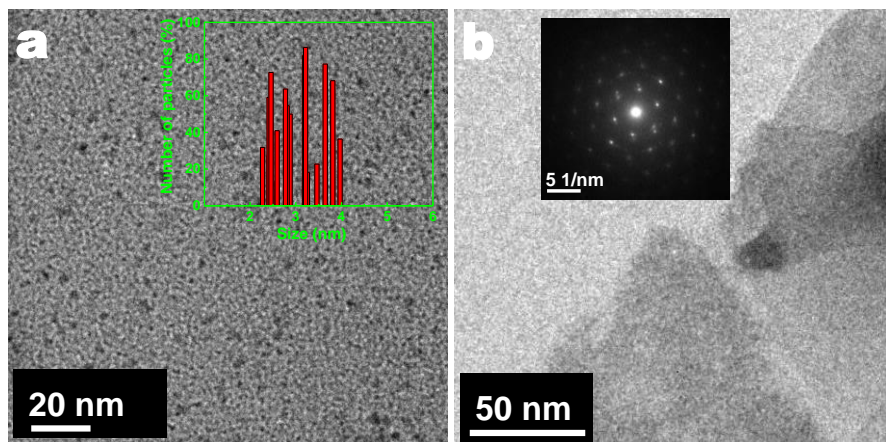


Fig. S10: TEM images of MoSe₂ nanocrystals electrophoretic deposited using 0.1 wt.% aq. BMImCl electrolyte. (a) showing nearly monodisperse particles of MoSe₂ with a narrow particle size distribution around 3.2 nm shown in the inset, and (b) shows the presence of coexisting crystalline nanosheets of MoSe₂, inset shows the hexagonal crystal lattice corresponding to semi-conducting 2H phase.

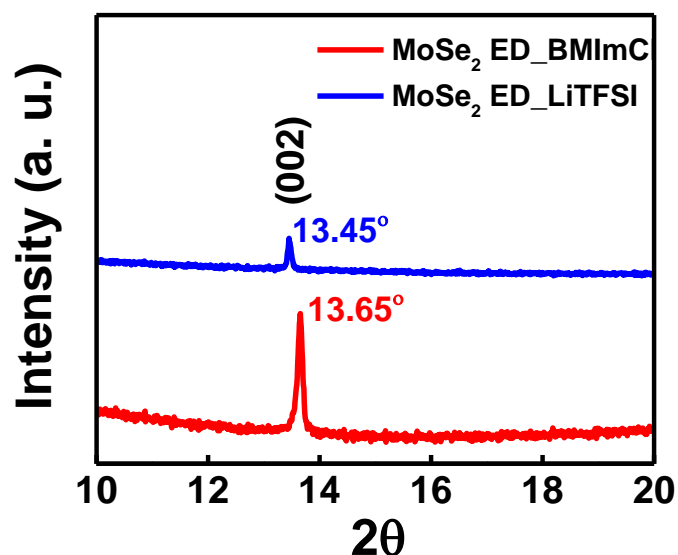


Fig. S11: Comparison of powder X-ray diffraction pattern of Electrophoretic deposited MoSe₂ nanocrystals using aq. LiTFSI and aq. BMImCl based electrolytes.

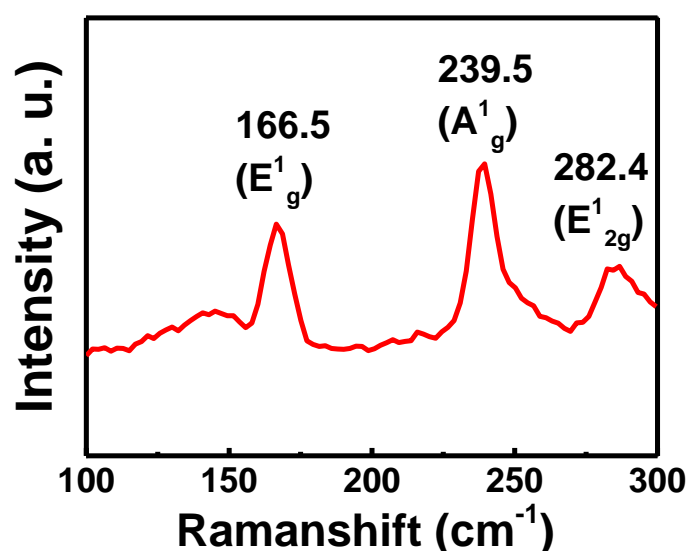


Fig. S12: Raman spectrum of MoSe₂ nanocrystals electrophoretic deposited using 0.1 wt.% aq. BMImCl electrolyte.

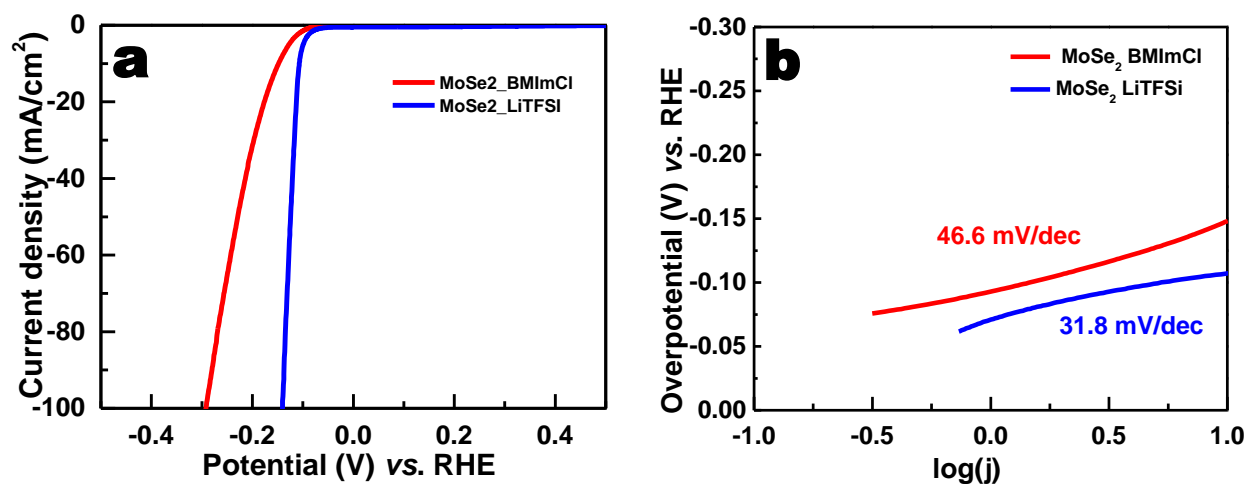


Fig. S13: Comparison of electrochemical performance of MoSe₂ nanocrystals with and without Li content prepared by electrochemical exfoliation and co-deposition using LiTFSI and no lithium containing BMImCl based aq. electrolyte.